First measurement of Timelike Compton Scattering

P.C., Silvia Niccolai, Stepan Stepanyan, the CLAS Collaboration

Published 22 December 2021: 10.1103/PhysRevLett.127.262501

Pierre Chatagnon
Jefferson Lab
pierrec@jlab.org

QNP 2022
5th-9th September 2022

Outline

- Introduction to the Generalized Parton Distributions
- Timelike Compton Scattering
- Jefferson Lab and the CLAS12 detector
- Analysis strategy and positron identification
- Results

The Generalized Parton Distributions

Understanding the inner structure of nucleons is challenging
→ Perturbative formalism not applicable to QCD at low energies

Form Factors
Position in the transverse plane

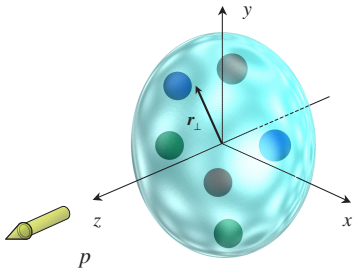

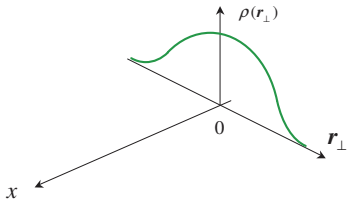

Accessed via elastic scattering

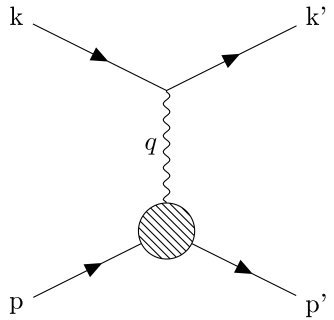

Generalized Parton Distributions

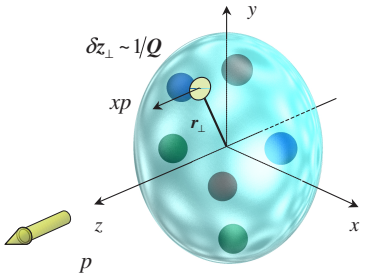

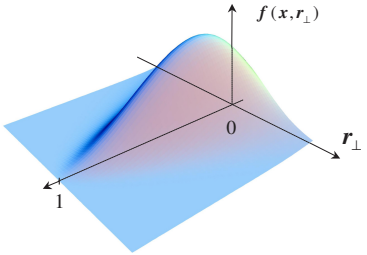

...and their **correlations**
Accessed in DVCS

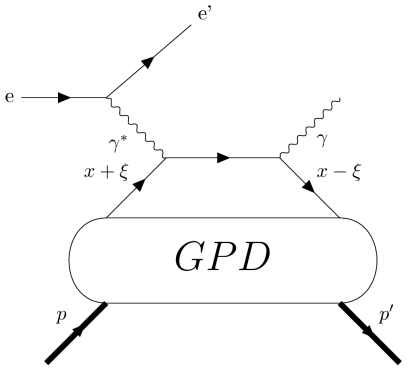

Parton Distribution Functions
Momentum in the longitudinal direction

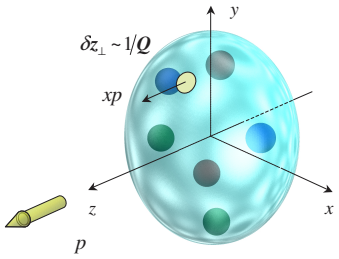

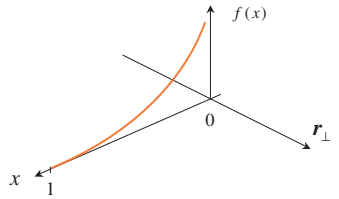

Accessed via **D**eep **I**nelastic **S**cattering

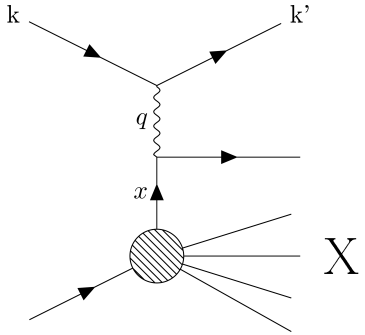

Figures in Belitsky, Radyushkin, *Physics Reports*, 2005

What can we learn from GPDs ?

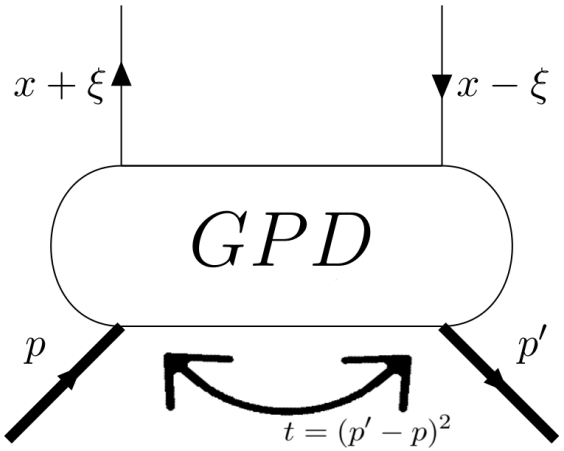

- **Tomography of the nucleon** The Fourier transform of the GPDs can be interpreted as a probability density:

$$H^q(x, b_\perp) = \int \frac{d^2\Delta_\perp}{(2\pi)^2} e^{-ib_\perp \Delta_\perp} H^q(x, 0, -\Delta_\perp^2)$$

Burkardt, *Int.J.Mod.Phys.A*, 2002

- **Spin puzzle**

$$\frac{1}{2} = J_Q + J_G$$

Ji's sum rule:

$$J_Q = \sum_q \frac{1}{2} \int_{-1}^{1} dx\ x(H^q(x,\xi,0) + E^q(x,\xi,0))$$

Ji, *Phys. Rev. Lett*, 1997

- **Mechanical properties**
Link to the Energy-Momentum Tensor (EMT) FFs

$$\int_{-1}^{1} dx\ xH^q(x,\xi,t) = A^q(t) + \xi^2 D^q(t)$$

$$\int_{-1}^{1} dx\ xE^q(x,\xi,t) = B^q(t) - \xi^2 D^q(t)$$

Polyakov, *Physics Letters B*, 2003

Timelike Compton Scattering

DVCS: $ep \to e'p'\gamma$ **TCS**: $\gamma p \to e^+e^-p'$

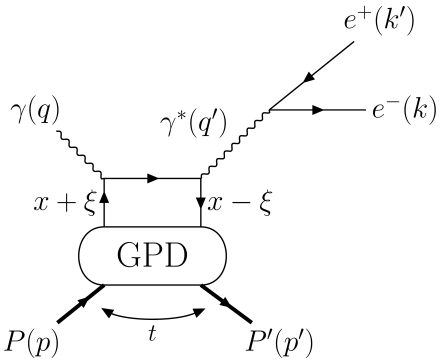

TCS (factorization regime $-t/Q'^2 \ll 1$)

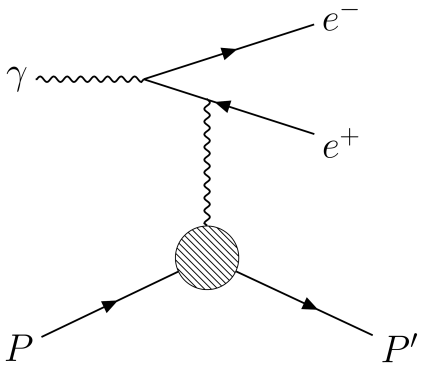

Bethe-Heitler

Kinematic definitions

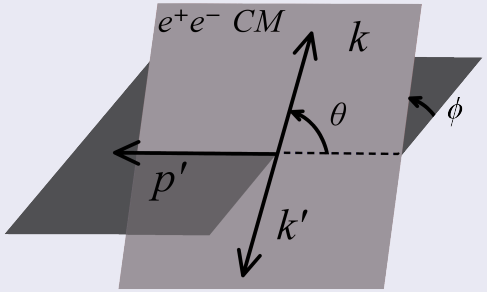

$t = (p - p')^2$
$Q'^2 = (k + k')^2$

- BH cross section only depends on electromagnetic FFs $\sigma_{BH} >> \sigma_{TCS}$ at JLab energies
- Unpolarized interference cross section Berger, Diehl, Pire, Eur.Phys.J.C23:675-689,2002

$$\frac{d^4\sigma_{INT}}{dQ'^2 dt d\Omega} \propto \frac{L_0}{L}\left[\cos(\phi)\frac{1+\cos^2(\theta)}{\sin(\theta)}\,\mathrm{Re}\tilde{M}^{--} + \ldots\right]$$

$$\to \tilde{M}^{--} = \frac{2\sqrt{t_0 - t}}{M}\frac{1-\xi}{1+\xi}\left[F_1\mathcal{H} - \xi(F_1+F_2)\tilde{\mathcal{H}} - \frac{t}{4M^2}F_2\mathcal{E}\right]$$

- Polarized interference cross section

$$\frac{d^4\sigma_{INT}}{dQ'^2 dt d\Omega} = \frac{d^4\sigma_{INT}\,|_{\mathrm{unpol.}}}{dQ'^2 dt d\Omega} - \nu\cdot A\,\frac{L_0}{L}\left[\sin(\phi)\frac{1+\cos^2(\theta)}{\sin(\theta)}\,\mathrm{Im}\tilde{M}^{--} + \ldots\right]$$

Both $\mathrm{Im}\mathcal{H}$ and $\mathrm{Re}\mathcal{H}$ can be accessed by TCS

Motivations to measure TCS

Test of universality of GPDs

- TCS is parametrized by GPDs
- **Comparison between DVCS and TCS** results allows to test the **universality** of GPDs (especially the imaginary part of $\mathcal{H}$)
- TCS does not involve Distribution Amplitudes unlike Deeply Virtual Meson Production
  $\rightarrow$ direct comparison between DVCS and TCS

Real part of CFFs and nucleon D-term

- $\mathrm{Re}\mathcal{H}$ is still not well constrained by existing data.

$$\mathrm{Re}\mathcal{H}(\xi,t) = \mathcal{P}\int_{-1}^{1} dx \left(\frac{1}{\xi - x} - \frac{1}{\xi + x}\right) \mathrm{Im}\mathcal{H}(\xi,t) + \Delta(t)$$

- $\Delta(t)$ related to the EM FF $D^Q(t)$, related to **mechanical properties** of the nucleon.

$$\Delta(t) \propto D^Q(t) \propto \int d^3\mathbf{r}\; p(r) \frac{j_0(r\sqrt{-t})}{t}$$

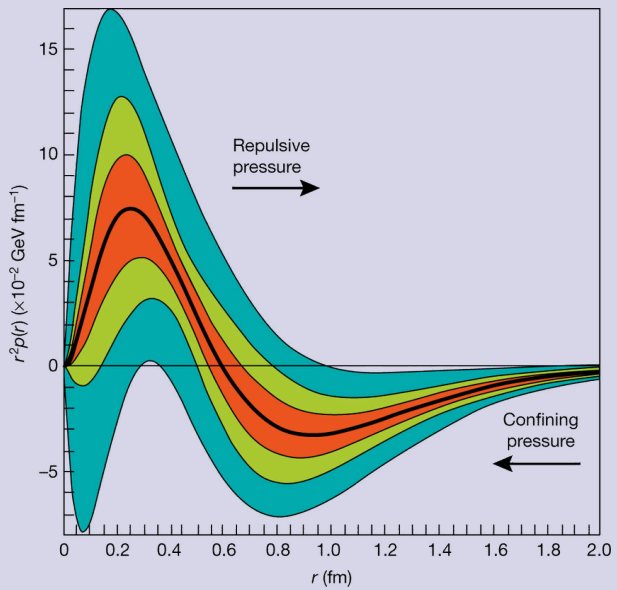

Burkert, Elouadrhiri, Girod. Nature 2018

Review in Polyakov, Schweitzer, International Journal of Modern Physics A, 2018

M.V. Polyakov. PLB, 2003

Experimental setup: CLAS12 at Jefferson Lab

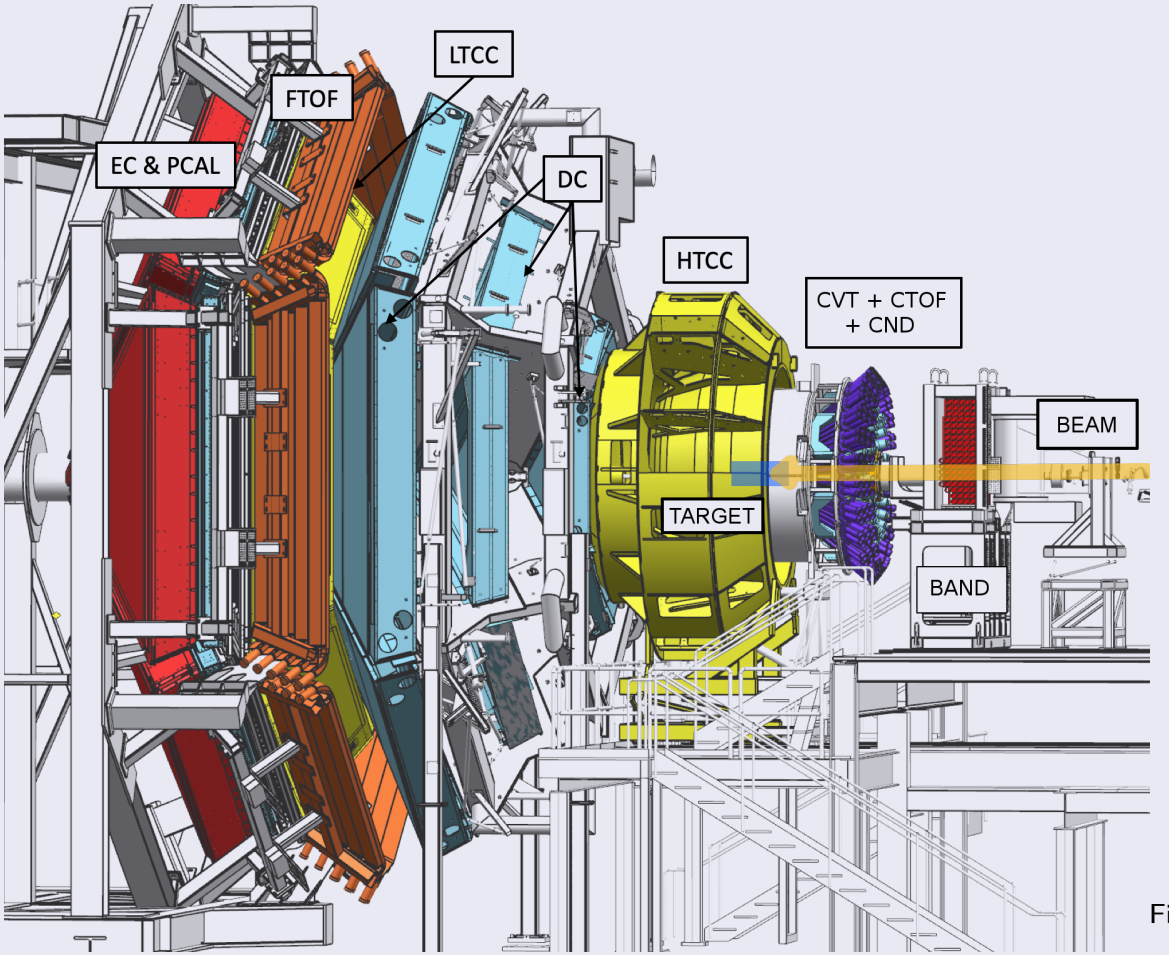

- **Forward Detector (6 sectors)**
  - Torus magnet
  - Drift Chambers
  - Forward Time-of-Flight
  - Calorimeters (EC and PCAL)
  - Cherenkov counters
- **Central Detector**
  - Solenoid magnet
  - Central Vertex Tracker (Silicon and micromegas)
  - Central Time-of-Flight
  - Central Neutron Detector

Figure in Burkert et al., *NIM A*, 2020

Data set used in this work

- **Fall 2018** run period
- ***LH*$_2$** target / **10.6 GeV** polarized e^- beam
- Inbending torus magnetic field
- Accumulated charge: $\sim$ 150 mC (200 fb^{-1})

Experimental setup: CLAS12 at Jefferson Lab

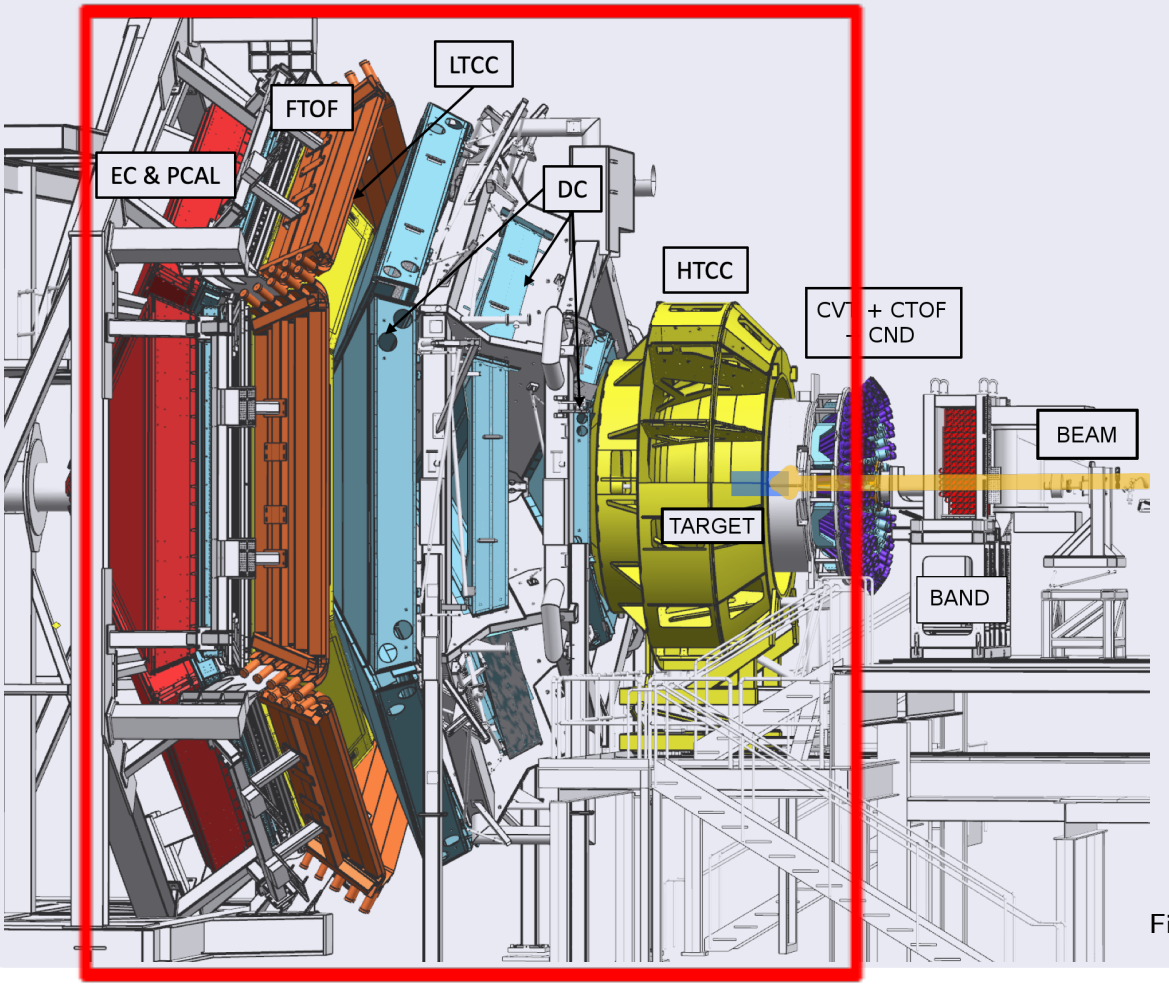

- **Forward Detector (6 sectors)**
  - Torus magnet
  - Drift Chambers
  - Forward Time-of-Flight
  - Calorimeters (EC and PCAL)
  - Cherenkov counters
- Central Detector
  - Solenoid magnet
  - Central Vertex Tracker (Silicon and micromegas)
  - Central Time-of-Flight
  - Central Neutron Detector

Figure in Burkert et al., *NIM A*, 2020

Data set used in this work

- **Fall 2018** run period
- LH_2 target / **10.6 GeV** polarized e^- beam
- Inbending torus magnetic field
- Accumulated charge: $\sim$ 150 mC (200 fb^{-1})

Experimental setup: CLAS12 at Jefferson Lab

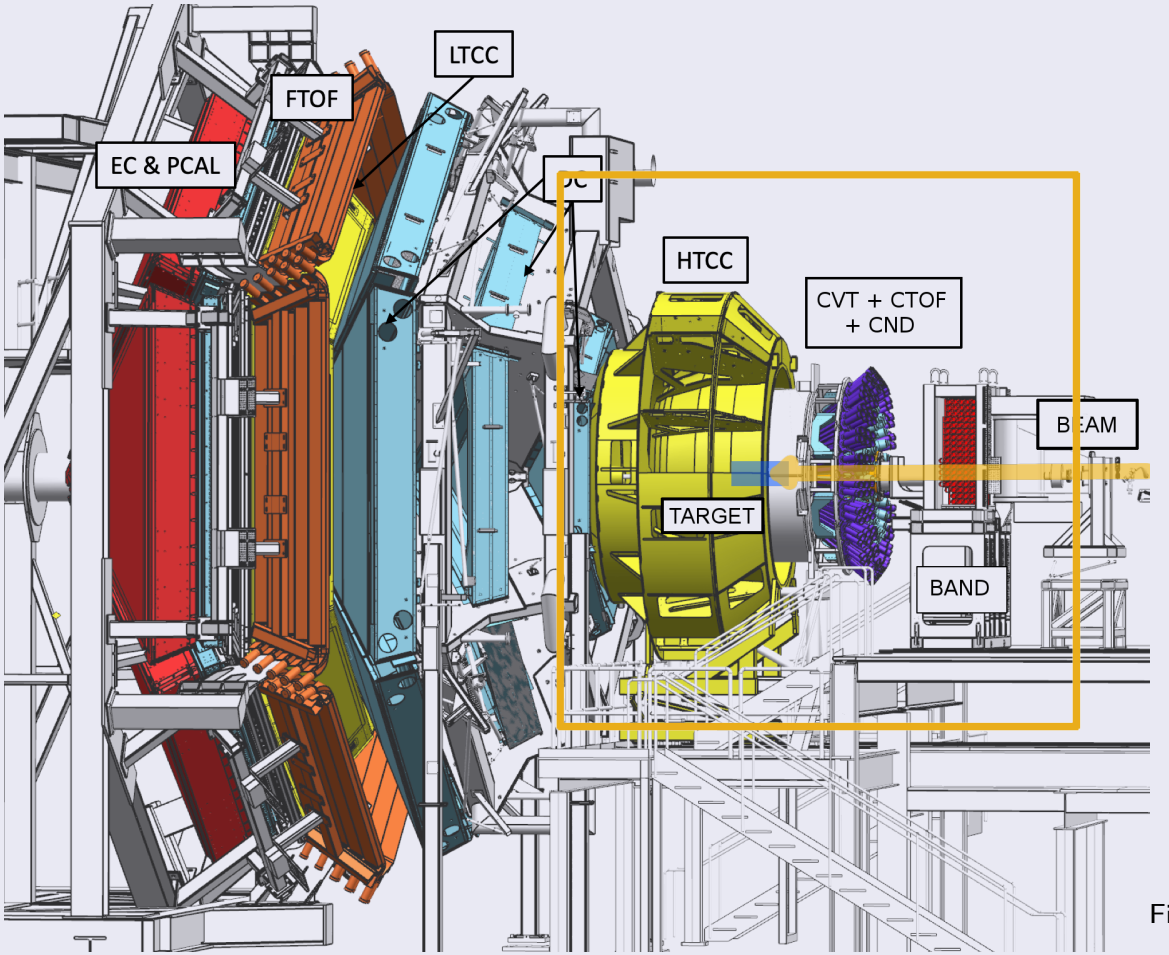

- **Forward Detector (6 sectors)**
  - Torus magnet
  - Drift Chambers
  - Forward Time-of-Flight
  - Calorimeters (EC and PCAL)
  - Cherenkov counters
- **Central Detector**
  - Solenoid magnet
  - Central Vertex Tracker (Silicon and micromegas)
  - Central Time-of-Flight
  - Central Neutron Detector

Figure in Burkert et al., *NIM A*, 2020

Data set used in this work

- **Fall 2018** run period
- ***LH*$_2$** target / **10.6 GeV** polarized e^- beam
- Inbending torus magnetic field
- Accumulated charge: $\sim$ 150 mC (200 fb^{-1})

Analysis strategy

CLAS12 PID + e^+ NN ID

$$e\ p \rightarrow (e')\gamma p \rightarrow (X)\ e^+ e^- p'$$

Exclusivity cuts

$p_X = p_{beam} + p_{target} - p_{e^+} - p_{e^-} - p_{p'}$

$|M_X^2| < 0.4\ \mathrm{GeV}^2$

Quasi-real photoproduction

$\frac{Pt_X}{P_X} < 0.05$

$\rightarrow Q^2 < 0.1\ \mathrm{GeV}^2$

after momentum corrections and fiducial cuts

Simulation

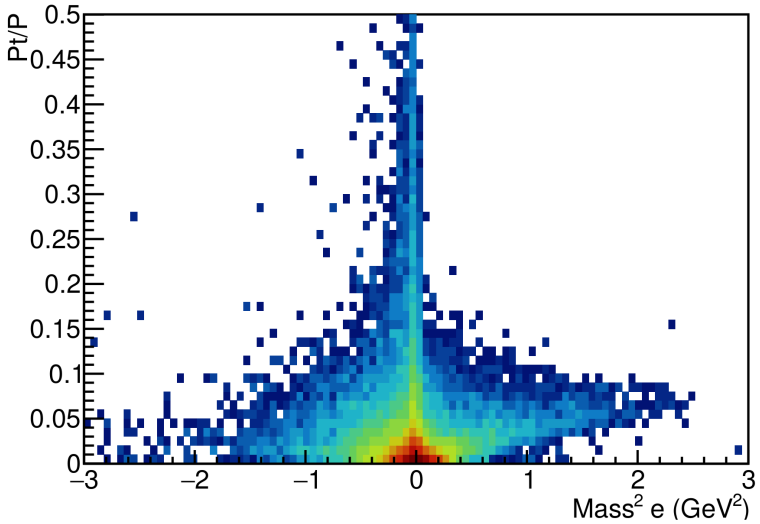

Data

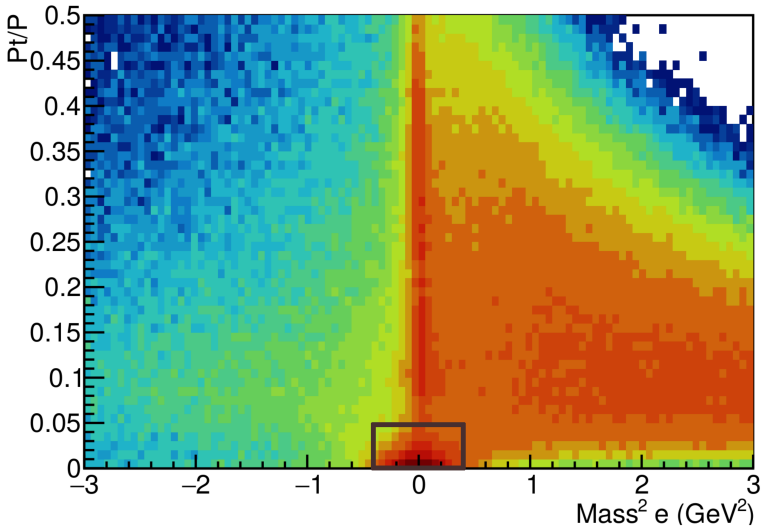

Positron identification

Above 4.5 GeV, the HTCC cannot distinguish positron from pions

Signal: e^+ identified as e^+ Background: π^+ identified as e^+

Strategy and discriminating variables: take advantage of the ECAL segmentation

Positron: electromagnetic shower Pion: Minimum Ionizing Particle (MIP)

$$SF_{\text{EC Layer}} = \frac{E_{dep}(\text{EC Layer})}{P} \qquad M_2 = \frac{1}{3}\sum_{U,V,W} \frac{\sum_{\text{strip}} (x-D)^2 \cdot \ln(E)}{\sum_{\text{strip}} \ln(E)} \rightarrow \textbf{6 variables}$$

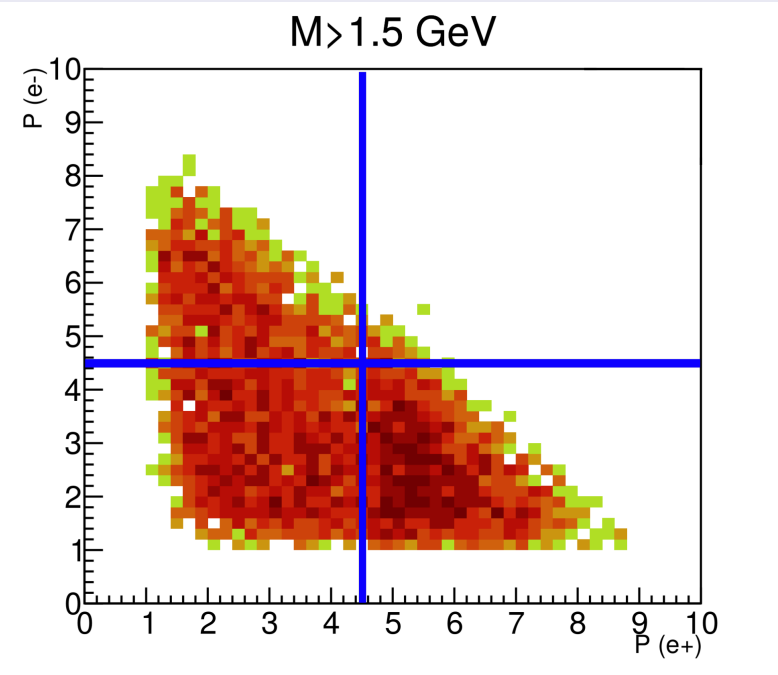

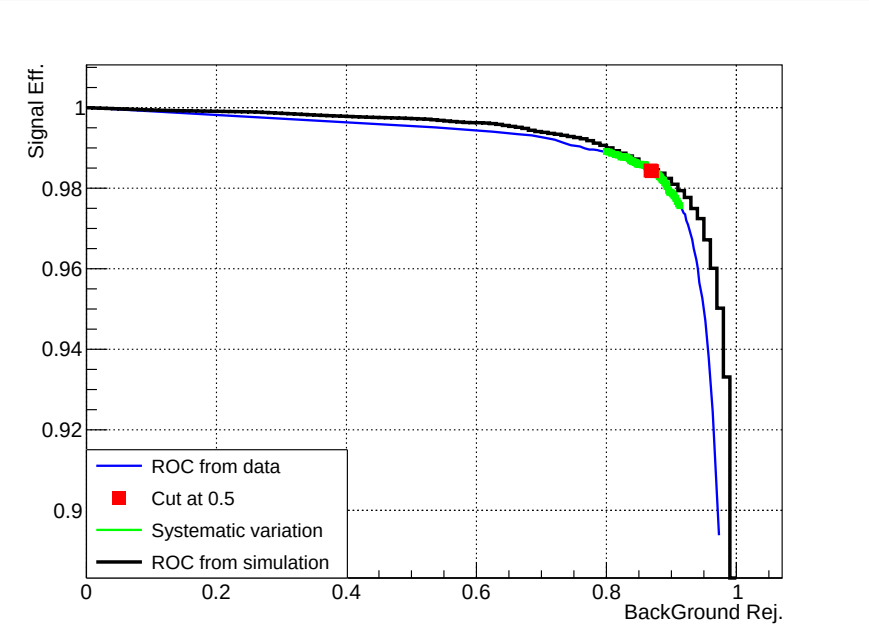

- Signal in data⇒ Outbending electrons
- Background in data⇒ $ep \rightarrow e\pi^+_{PID=e^+}(n)$

B/S: 50% → 5% for $P_{e^+} > 4.5$ GeV

Data/Simulation comparison

Phase space of interest

- $0.15\ \mathrm{GeV}^2 < -t < 0.8\ \mathrm{GeV}^2$
- $1.5\ \mathrm{GeV} < M_{e^+e^-} < 3\ \mathrm{GeV}$
- $4\ \mathrm{GeV} < E_\gamma < 10.6\ \mathrm{GeV}$

Observations

- Vector mesons peaks are visible in data: ω (770 MeV), ρ (782 MeV), Φ (1020 MeV) and J/ψ (3096 MeV)
- Data/simulation are matching at 15 % level, up to normalization factor. No evident high mass vector meson production (ρ (1450 MeV, 1700 MeV)

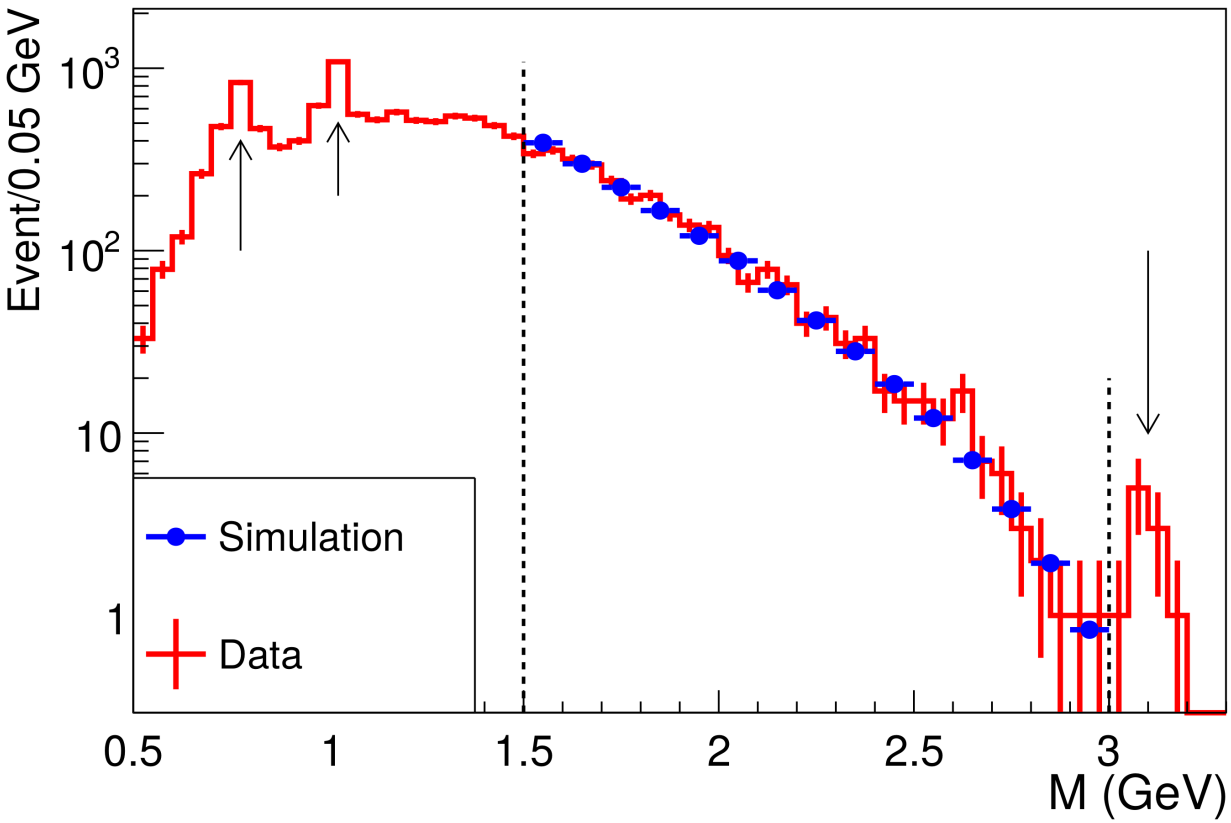

Observable 1: Photon polarization asymmetry ($A_{\odot U}$)

Definition

$$A_{\odot U} = \frac{d\sigma^+ - d\sigma^-}{d\sigma^+ + d\sigma^-} = \frac{-\frac{\alpha_{em}^3}{4\pi s^2}\frac{1}{-t}\frac{m_p}{Q'}\frac{1}{\tau\sqrt{1-\tau}}\frac{L_0}{L}\sin\phi\,\frac{(1+\cos^2\theta)}{\sin(\theta)}\,\mathrm{Im}\tilde{M}^{--}}{d\sigma_{BH}}$$

Experimental measurement

- $A_{\odot U}(-t, E\gamma, M; \phi) = \frac{1}{P_b}\frac{N^+ - N^-}{N^+ + N^-}$ where $N^{\pm} = \sum \frac{1}{Acc} P_{trans.}$
- $P_{trans.}$ is the **transferred polarization** from the **electron to the photon**, fully calculable in QED

  Olsen, Maximon, Phys. Rev.114 (1959)
- P_b is the **polarization of the CEBAF** electron beam (85%)
- The ϕ-distribution is fitted with a sine function

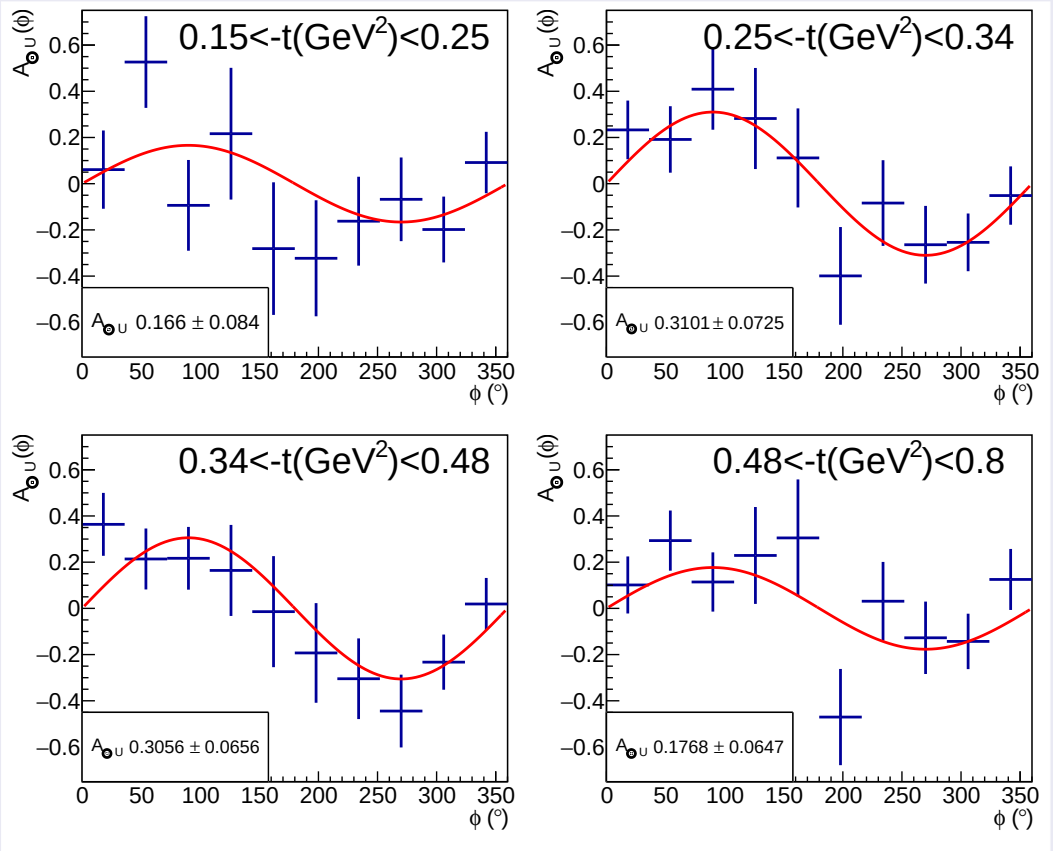

$A_{\odot U}$ results

- A **sizeable asymmetry** is measured (above the expected vanishing $A_{\odot U}$ of BH)
  $\rightarrow$ **signature of TCS**
- Theoretical predictions were provided by M.Vanderhaeghen, JGU Mainz (VGG model) and P.Sznajder, NCBJ Warsaw (GK model)
- Size of the asymmetry is **well reproduced** by VGG and GK models
  $\rightarrow$ **model dependent hints for universality of GPDs**

$< M >= 1.8$ GeV; $< E_\gamma >= 7.29$ GeV; $< \theta >= 92^\circ$

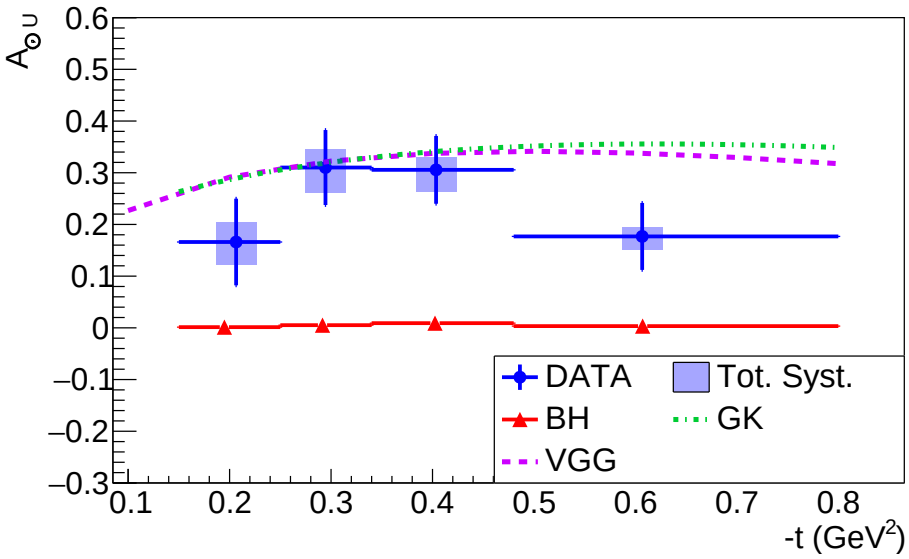

Observable 2: Forward-Backward asymmetry

- Use the different parity of the TCS and BH amplitudes under the inversion of the leptons directions

$$k \leftrightarrow k' \iff (\theta, \phi) \leftrightarrow (180^\circ - \theta, 180^\circ + \phi)$$

BH cross section

$$\frac{d\sigma_{BH}}{dQ^2\, dt\, d\Omega} \propto \frac{1+\cos^2\theta}{\sin^2\theta} \xrightarrow{FB} \frac{d\sigma_{BH}}{dQ^2\, dt\, d\Omega}$$

Int. cross section

$$\frac{d^4\sigma_{INT}}{dQ'^2 dt d\Omega} \propto \frac{L_0}{L} cos(\phi) \frac{1+cos^2(\theta)}{sin(\theta)} \xrightarrow{FB} -\frac{d\sigma_{INT}}{dQ^2\, dt\, d\Omega}$$

A_{FB} formula

$$A_{FB}(\theta_0, \phi_0) = \frac{d\sigma(\theta_0, \phi_0) - d\sigma(180^\circ - \theta_0, 180^\circ + \phi_0)}{d\sigma(\theta_0, \phi_0) + d\sigma(180^\circ - \theta_0, 180^\circ + \phi_0)} = \frac{-\frac{\alpha_{em}^3}{4\pi s^2} \frac{1}{-t} \frac{m_p}{Q'} \frac{1}{\tau\sqrt{1-\tau}} \frac{L_0}{L} \cos\phi_0 \frac{(1+\cos^2\theta_0)}{\sin(\theta_0)} \mathrm{Re}\tilde{M}^{--}}{d\sigma_{BH}(\theta_0, \phi_0) + d\sigma_{BH}(180^\circ - \theta_0, 180^\circ + \phi_0)}$$

Integration over forward angular bin: $\theta \in [50^\circ, 80^\circ]/\phi \in [-40^\circ, 40^\circ]$

- Concept initially explored for J/Ψ production
  Gryniuk, Vanderhaeghen, *Phys. Rev. D*, 2016.
- Exploratory studies for TCS performed alongside this work, during my thesis.
- Predictions for TCS have been published very recently + **LO radiative correction negligible**
  Heller, Keil, Vanderhaeghen, *Phys. Rev. D*, 2021.

A_{FB} results

- A_{FB} measured in two mass regions: $M \in [1.5\ \mathrm{GeV}, 3\ \mathrm{GeV}]$ and $M \in [2\ \mathrm{GeV}, 3\ \mathrm{GeV}]$
- The measured A_{FB} is non-zero: **evidence for signal** beyond pure BH contribution
- Three model predictions
  1. VGG without D-term
  2. VGG with D-term

     D-term in Pasquini et al., *Physics Letters B*, 2014
  3. GK without D-term
- Measured asymmetry is better reproduced by the VGG model **including the D-term** in both mass bins

  → importance of the D-term in the parametrization of GPDs

  → TCS is a prime reaction to constrain the D-term

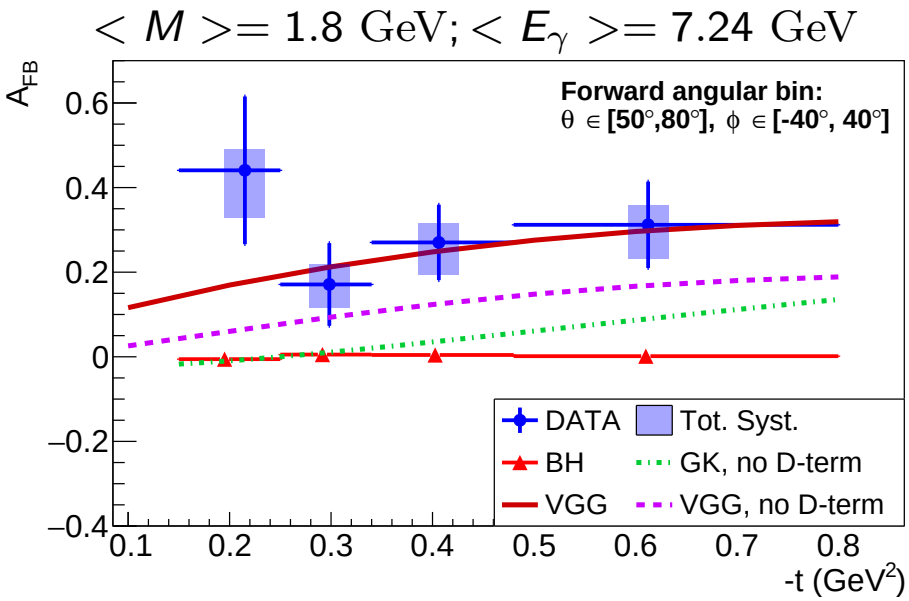

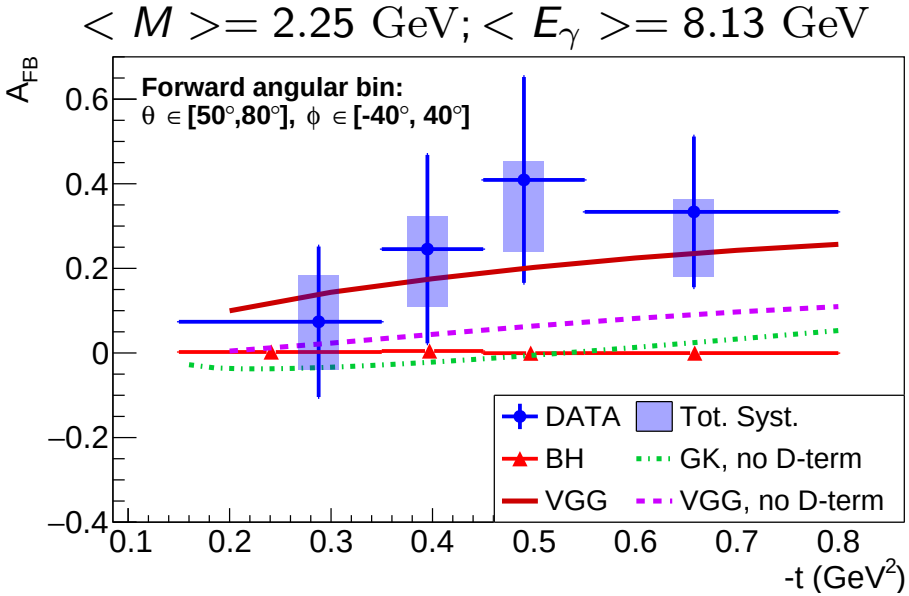

Conclusions

Takeaways

- TCS observables were measured for the **first time**
- Sizeable $A_{\odot U}$ (sensitive to Im$\mathcal{H}$) and A_{FB} (sensitive to Re$\mathcal{H}$) are **clear signatures of TCS**
- The results obtained allow to draw physical conclusions:
  - the $A_{\odot U}$ is well reproduced by models that reproduce existing DVCS data
    $\rightarrow$ hints for **universality of GPDs**
  - the Forward/Backward asymmetry appears to be better reproduced by model with a D-term
    $\rightarrow$ promising path to the measurement of the D-term
    $\rightarrow$ access to the **mechanical properties of the proton**

Opportunities ahead to measure TCS:

- EIC, Ultra-peripheral collisions (LHC) $\rightarrow$ test QCD NLO corrections
  Mueller,Pire,Szymanowski,Wagner, PRD, 2012
- CLAS12 high lumi/high energy upgrades $\rightarrow$ improve constraints on D-term

PRL article: 10.1103/PhysRevLett.127.262501

Direct access to the TCS article

Back Up

Acceptance

Acceptance calculation using BH-weighted events

$$Acc_{\mathcal{B}} = \frac{N_{\mathcal{B}}^{REC}}{N_{\mathcal{B}}^{GEN}} \qquad N_{\mathcal{B}}^{REC} = \sum_{REC \in \mathcal{B}} Eff_{corr}\ w \qquad N_{\mathcal{B}}^{GEN} = \sum_{GEN \in \mathcal{B}} w$$

Multidimensional binning of the acceptance

4 bins in $-t$, 3 bins in E_γ and Q'^2, 10° x 10° bins in the ϕ/θ plane. Bins with $\frac{\Delta Acc}{Acc} > 0.5$ and $Acc < 0.05$ are discarded (ΔAcc is statistical error).

Large region with no acceptance
($\phi \sim 0^\circ/\theta \sim 180^\circ$ and $\phi \sim 180^\circ/\theta \sim 0^\circ$)

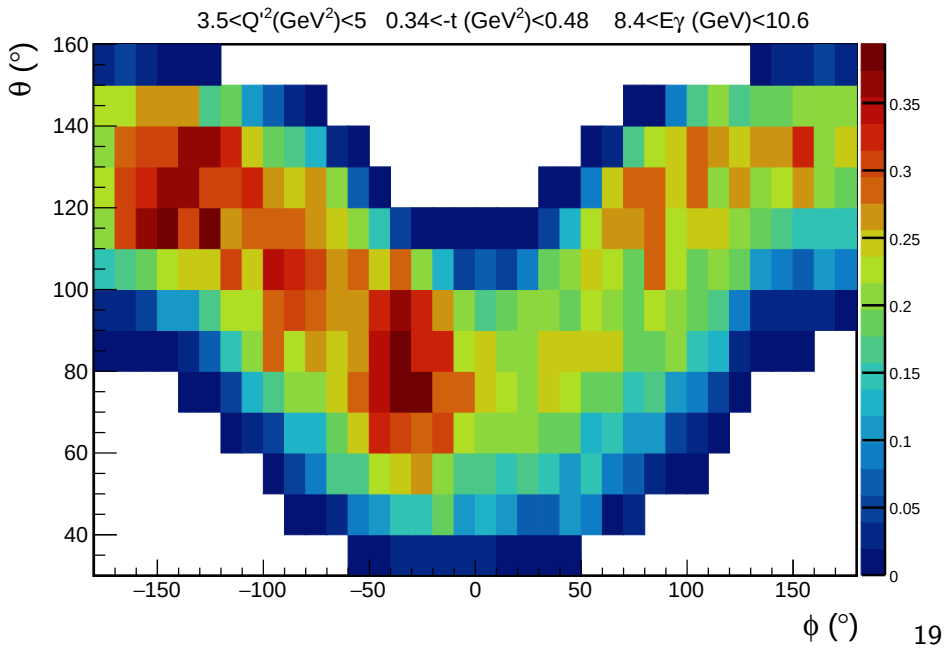

Efficiency corrections

- **Data-driven correction** for the proton detection efficiency derived using $ep \to e'\pi^+\pi^-(p')$ reaction
- Efficiency correction from **background merging** using random trigger events

Positron identification

Above 4.5 GeV, the HTCC cannot distinguish positron from pions

Signal: e^+ identified as e^+ Background: π^+ identified as e^+

Strategy and discriminating variables: take advantage of the ECAL segmentation

Positron: electromagnetic shower Pion: Minimum Ionizing Particle (MIP)

$$SF_{\text{EC Layer}} = \frac{E_{dep}(\text{EC Layer})}{P} \qquad M_2 = \frac{1}{3}\sum_{U,V,W} \frac{\sum_{\text{strip}}(x-D)^2 \cdot \ln(E)}{\sum_{\text{strip}} \ln(E)} \rightarrow \textbf{6 variables}$$

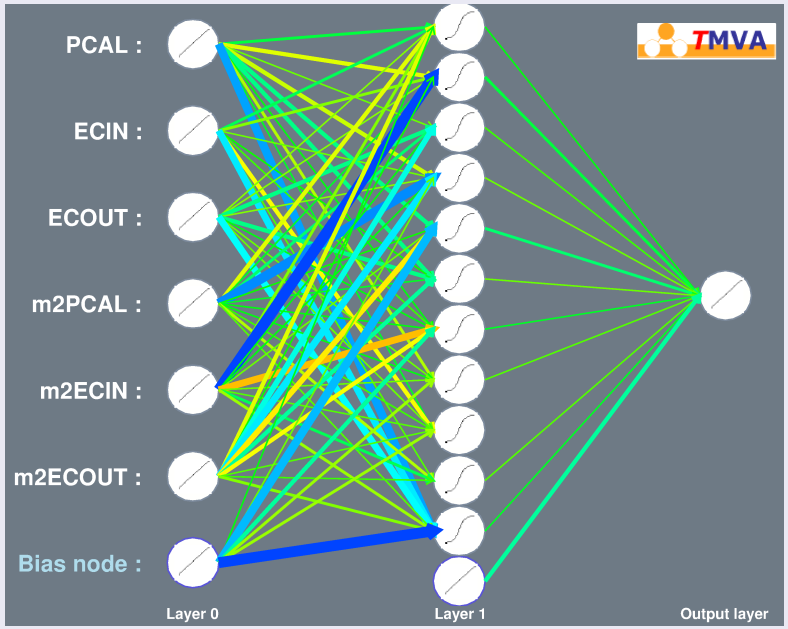

Output: Signal $\rightarrow$ 1 Background $\rightarrow$ 0

B/S from 50% to 5%

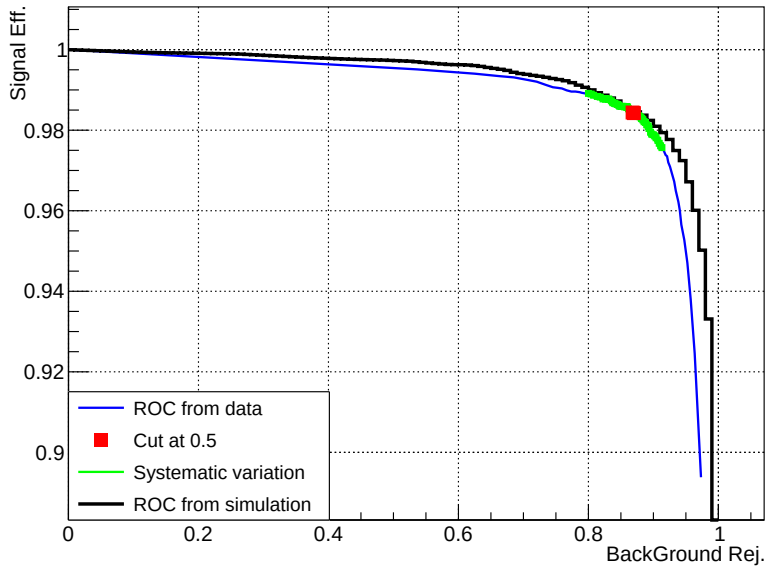

- Signal in data$\Rightarrow$ Outbending electrons
- Background in data$\Rightarrow$ $ep \rightarrow e\pi^+_{PID=e^+}(n)$

Systematics

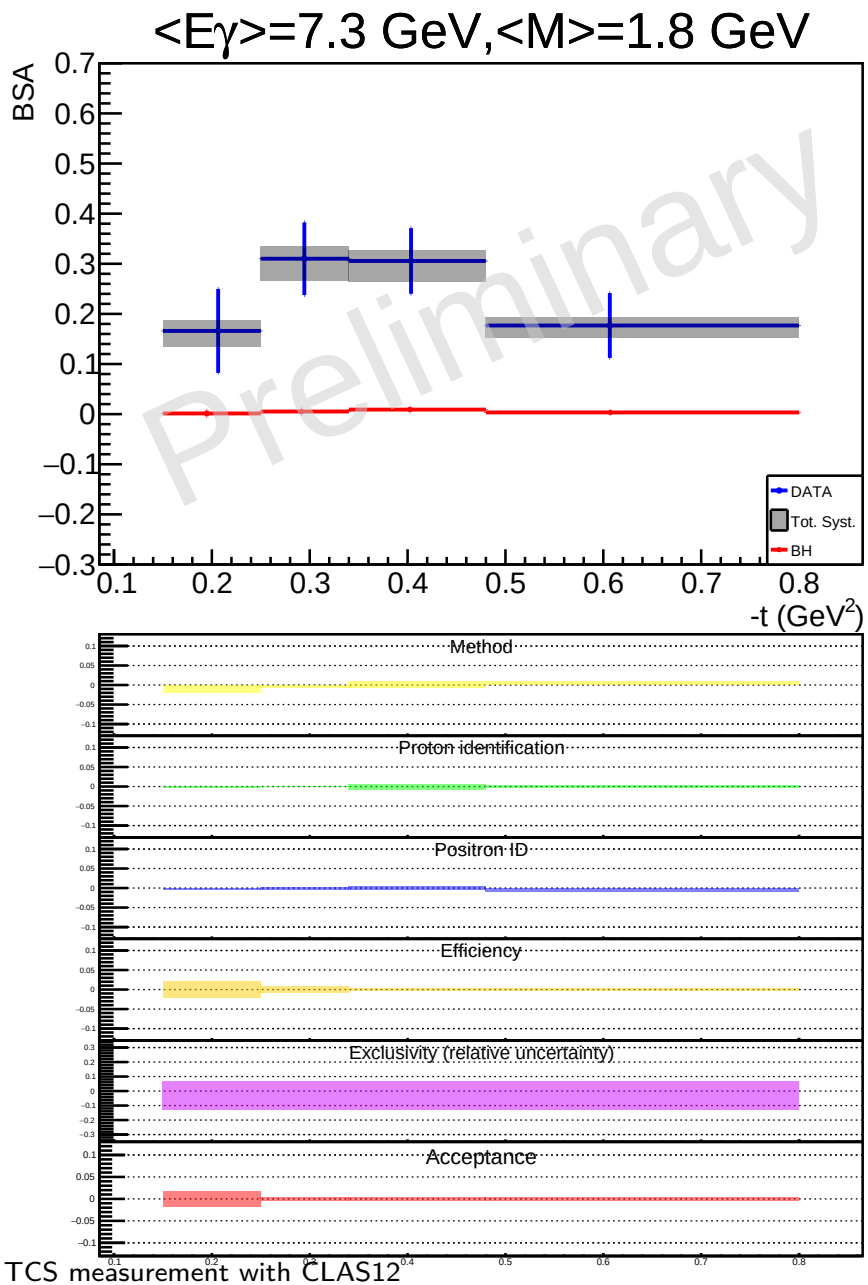

Method

- Calculated from generated BH events, and full-chain simulated events.

Proton

- Apply χ^2 cut for the proton identification

Positron Identification

- Vary the positron ID cut (0.5 ± 0.3; max. significance region)

Efficiency

- Calculate observable with/without data-driven proton efficiency

Exclusivity cuts

- Vary the values of the exclusivity cuts: $| Pt/P | < 0.05 \pm 0.01$, $| M_X^2 | < 0.4 \pm 0.1\ \mathrm{GeV}^2$

Fully integrated relative uncertainty

Acceptance

- Calculate observable with acceptance produced using BH-weighted events or unity weights

- Neighboring bins uncertainties are averaged
- Then added in quadrature